Article:
Aksornniem, Suttipan, Evans, Richard F L, Chantrell, Roy W. et al. (2016) Magnetic Switching in BPM, TEAMR, and Modified TEAMR Using Dielectric Underlayer Media. IEEE Transactions on Magnetics. 7298448. ISSN: 1941-0069

https://doi.org/10.1109/TMAG.2015.2490626

Magnetic Switching in BPM, TEAMR, and Modified TEAMR by Using Dielectric Underlayer Media

Suttipan Aksornniem[1,2], Richard F. L. Evans[2], Roy W. Chantrell[2], Rardchawadee Silapunt[1]

[1]Department of Electronic and Telecom. Eng., King Mongkut's University of Technology Thonburi, Bangkok, 10140, Thailand
[2]Department of Physics, University of York, Heslington, York, YO10 5DD, UK

In this paper we study the coercivity of Bit Patterned Media (BPM), Trapping Electron Assisted Magnetic Recording (TEAMR), and modified TEAMR media by using a dielectric underlayer. The VAMPIRE magnetic simulator is used to model 3 structures of recording bits and to study the M-H loops using an atomistic spin model. The results show that the magnetic switching reduction in modified TEAMR and TEAMR depends on the bit size. The percentage of magnetic switching reduction in modified TEAMR is also larger than TEAMR for all bit sizes. For a bit size of 1.6×1.6×3.2 nm^3, the percentage of magnetic switching reduction in modified TEAMR is approximately 4 times higher than that in TEAMR.

***Index Terms*—magnetic data storage device; electron trapping assisted recording; TEAMR; VAMPIRE magnetic simulator; atomistic spin model.**

I. Introduction

HARD DISK drives are currently used to store over 90% of the world's digital data [1]. One main advantage of magnetic data storage is a much lower cost compared to any other technology, being approximately four times cheaper than equivalent solid state storage [2]. Recent developments in hard disk drives have seen improved areal density and energy efficiency. Presently, Perpendicular Magnetic Recording (PMR) technology is the dominant technology used in hard disk drives. However the areal density of conventional PMR is running into a limit of around 1 Tbpsi [3]. Areal density is limited by the requirement to retain thermal stability of written bits. Thermal stability cannot be maintained if the grain size is reduced below a critical limit where the magnetic anisotropy energy (K_uV/k_BT) is less than 60 [4]. The V and K_u represent the grain volume and magnetic anisotropy energy of the recording media respectively, k_B is the Boltzmann constant and T is the temperature. To obtain high thermal stability, the recording medium should have a high magnetic anisotropy energy. A favored candidate material is $L1_0$ ordered FePt with $K_u = 7\times10^6$ J/m^3 [5-6]. However, for such high anisotropy values the associated magnetic field required to write the data is greater than that available in conventional write heads.

Novel recording methods have been suggested to reduce the coercivity of the medium during the writing process. Examples include Microwave Assisted Magnetic Recording (MAMR) [7], Heat Assisted Magnetic Recording (HAMR) [8], and Exchange Coupled Composite (ECC) media [9]. Here we study Trapping Electron Assisted Magnetic Recording (TEAMR) [10]. Previously, trapping electron effect was demonstrated in CoCrPt-TiO_2 [11]. A low voltage (3 V_{dc}) was sufficient to create an electric field strong enough to trap 0.15 electron per cobalt atom in grain boundaries of media. That can reduce 13% of applied magnetic field reduction [11]. In addition, the first demonstration of electric field modified FePt properties in [12] showed that the magnetocrystalline anisotropy of FePt can be changed by an applied electric field. The method works by inducing electron filling in the valence band of $L1_0$ ordered FePt by applying a dc-voltage during the writing process [10] resulting in a change of the bandfilling to an effective number of electrons n_{eff}. By using Density Functional Theory (DFT) calculations [10] of the electron filling it was found that n_{eff} = 18.38 for $L1_0$ ordered FePt reduces the magnetic anisotropy energy (K_u) to zero. It was also found in [10] that the saturation magnetization (M_S) depended on n_{eff}. Recently [13] the alloying approach was studied theoretically using DFT, giving very good agreement with experimental data. In [13] the approach used was to model the actual alloy structures including structural relaxation. This goes beyond rigid the band model of [10] and suggests that the alloying approach does not give the exact dependence of K_u on n_{eff} in relation to TEAMR.

Recent simulations of TEAMR using finite element simulations demonstrated the capability of an electric field to induce electron filling in $L1_0$ ordered FePt [10]. However, it was found that the electric field gives rise to a rather localized change in the magnetocrystalline anisotropy. The calculations showed that bandfilling enhancement in a TEAMR structure only occurs close to the surface of an $L1_0$ ordered FePt recording bit because $L1_0$ ordered FePt is a conductor. Applying an external field directly makes it difficult to add electrons deep within the $L1_0$ ordered FePt film and so this effect can only reduce the anisotropy on the top surface of the bit. Therefore the reduction of the magnetic switching field was found to be only around 10%. A revised recording method known as modified TEAMR (M-TEAMR) uses a dielectric layer to induce surface charges at the side of the grain [14]. Using a finite element simulator it was predicted that the electron bandfilling increased deep inside the $L1_0$ ordered FePt layer. Although the bandfilling remains localized to the intergranular dielectric layer, the magnetocrystalline anisotropy is reduced within a larger volume of the grain than with normal TEAMR.

Here we study the magnetic switching of $L1_0$ ordered FePt bit patterned media (BPM), using TEAMR, and M-TEAMR

Manuscript received xx x, xxxx; revised xx x, xxxx; accepted xx x, xxxx. Date of publication xx x, xxxx; date of current version xx x, xxxx.
Corresponding author: R. Silapunt (e-mail: rardchawadee.sil@kmutt.ac.th).
Color versions of one or more of the figures in this paper are available online at http://ieeexplore.ieee.org.

by introducing a dielectric underlayer. The magnetic switching of the 3 structures is investigated using an atomistic spin model, which has the required spatial resolution to investigate the effects of local reduction of the magnetocrystalline anisotropy.

II. Theoretical Model

The magnetic properties are investigated using an atomistic spin model [15] where the energetics of the system are described by the following spin Hamiltonian ($\mathcal{H}$).

$$\mathcal{H} = \mathcal{H}_{exc} + \mathcal{H}_{ani} + \mathcal{H}_{app} \tag{1}$$

Denoting terms for the exchange interaction, magnetic anisotropy, and externally applied magnetic field respectively. The bulk material parameters are chosen to be representative of $L1_0$ ordered FePt, a strong candidate for next generation magnetic recording technology [16]. The contributions to the Hamiltonian, given below, consist of terms representing exchange in the Heisenberg form, uniaxial anisotropy and a Zeeman term giving the interaction with the externally applied field.. These terms are;

$$\mathcal{H}_{exc} = -\sum_{i \neq j} J_{ij} \hat{S}_i \cdot \hat{S}_j \tag{2}$$

$$\mathcal{H}_{ani}^{uni} = k_u \sum_i (\hat{S}_i \cdot \hat{e}_i)^2 \tag{3}$$

$$\mathcal{H}_{app} = -\sum_i \mu_s \hat{S}_i \cdot \hat{H}_{app} \tag{4}$$

where J_{ij} = 3.28×10^{-21} J/link is the nearest neighbor exchange interaction, $\hat{S}_i$ and $\hat{S}_j$ are unit vectors representing the local and neighboring spin directions, k_u is the uniaxial anisotropy constant, μ_s is the atomic spin moment, and $\hat{H}_{app}$ is the externally applied field. The effect of bandfilling is modeled by considering its effect on the local anisotropy and atomic spin moment [10].

We carry out calculations using the VAMPIRE atomistic modelling package [17], in which the magnetization dynamics of the system are included via the use of the LLG equation given by;

$$\frac{\partial \hat{S}_i}{\partial t} = -\frac{\gamma_i}{(1+\lambda_i^2)} (\hat{S}_i \times (\hat{H}_i + \lambda_i \hat{S}_i \times \hat{H}_i)) \tag{5}$$

Here λ_i and γ_i are the microscopic thermal bath coupling parameter and the gyromagnetic ratio respectively. The effective field on each spin is then given by $-d\mathcal{H}/dS_i$ where S_i is the magnetic moment of the site, *i*. To introduce the effects of temperature the local field is enhanced by a stochastic term, which describes the coupling of the spin system to the external thermal bath. The thermal fluctuations are included as a white noise term, uncorrelated in time and space, which is added into the effective field [18]. The stochastic integrals are interpreted as Stratonovich integrals [19]. The moments of the stochastic process are defined through fluctuation dissipation theory as:

$$\left\langle \varsigma_i^a(t) \varsigma_j^b(t) \right\rangle = 2\delta_{ij}\delta_{ab}(t-t') \frac{\lambda_i k_B T}{\mu_i \gamma_i} \tag{6}$$

$$\left\langle \varsigma_i^a(t) \right\rangle = 0 \tag{7}$$

Here *a, b* are Cartesian components and *T* is the temperature of the thermal bath to which the spins are coupled. The coupling of the spins to the thermal bath (λ_i) is a parameter which attempts to describe all of the energy and momentum transfer channels into the spin system, for example from the conduction electrons or the lattice.

This paper studies the coercivity of magnetic recording media of 3 structural types. These are BPM, TEAMR, and M-TEAMR including a dielectric underlayer. The 3 structures are shown in figure 1(B), 1(C), and 1(D). Figure (C) and (D) illustrate the major difference between TEAMR and M-TEAMR where coloring indicates the parts of the grain where the anisotropy is reduced due to the bandfilling. A recording grain consists of several unit cells of $L1_0$ ordered FePt. The cell size of $L1_0$ ordered FePt is 3.864 Å (c/a =0.96) that is shown in figure 1(A).

The aim is to investigate the effect on the coercivity of the degree of bandfilling, the width/thickness ratio (*W/t*) of the bits and the thermal stability value.

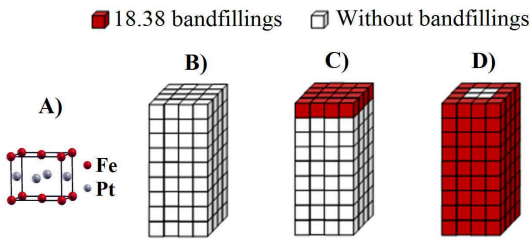

Fig. 1. Structures of A) $L1_0$ ordered FePt unit cell, B) BPM, C) TEAMR, and D) M-TEAMR by using dielectric underlayer, where the coloring indicates the parts of the grain where the anisotropy is reduced due to the bandfilling.

The recording bit of a BPM structure consists of many $L1_0$ ordered FePt unit cells that is shown schematically in figure 1(B). The bandfilled electron unit cells in the TEAMR structure (indicated by the colored cells) only occur at the top surface of $L1_0$ ordered FePt bit while the M-TEAMR structure gives rise to bandfilling at the side surface of the $L1_0$ ordered FePt grain. TEAMR and M-TEAMR structures are shown in figure 1(C) and 1(D), respectively. The material parameters used in the simulations are given in table I. Note that the exchange energy is independent of a number of bandfilling electron but on Boltzmann's constant and a number of nearest neighbor atoms.

K_u without bandfilling in $L1_0$ ordered FePt is 8.57×10^6 J/m^3 and with n_{eff} = 18.38 in $L1_0$ ordered FePt, the value decreases to zero. The saturation magnetizations (M_s) are 1.0745×10^6 J/(T·K^3) and 1.025×10^6 J/(T·K^3) without and with 18.38 electron bandfilling in $L1_0$ ordered FePt [10], respectively.

TABLE I
MATERIAL PROPERTIES

Parameter	Material:$L1_0$ ordered FePt	
	No bandfilling	18.38 bandfilling
Unit cell size, a	3.864 Å	3.864 Å
Unit cell size, c	3.748 Å	3.748 Å
Anisotropy energy	$1.2\text{x}10^{-22}$ J/atom	0 J/atom
Exchange energy	$3.28\text{x}10^{-21}$ J/link	$3.28\text{x}10^{-21}$ J/link
Atomic spin moment, μ_S	$1.62\mu_B$	$1.56\mu_B$

TABLE II
PARAMETERS AT DIFFERENT BANDFILLING

Bandfilling (e)	Material properties			
	K_u (J/m^3)	M_s (J/T·m^3)	μ_S (μ_B)	k_u (J/atom)
18.0	8.57×10^{6}	1.0745×10^{6}	1.620	1.198×10^{-22}
18.1	7.75×10^{6}	1.0631×10^{6}	1.603	1.084×10^{-22}
18.2	5.96×10^{6}	1.0528×10^{6}	1.588	8.337×10^{-23}
18.3	4.25×10^{6}	1.0431×10^{6}	1.573	5.945×10^{-23}
18.4	-0.47×10^{6}	1.0314×10^{6}	1.556	-6.575×10^{-24}
18.5	-1.64×10^{6}	1.0157×10^{6}	1.532	-2.294×10^{-23}
18.6	-1.29×10^{6}	0.9975×10^{6}	1.505	-1.804×10^{-23}

First we simulate different levels of electron bandfilling in TEAMR and modified TEAMR structures. The recording bits of TEAMR and modified TEAMR are modeled using the VAMPIRE simulator based on figure 1(C) and 1(D) respectively. The bit size is taken as 4×4×8 cells per bit (1.6×1.6×3.2 nm^3) in both structures. The initial simulations are carried out at 0K, which will allow comparison with micromagnetic simulations, followed by an investigation of the effect of temperature. The anisotropy and M_s values are calculated for electron bandfillings of n_{eff} = 18.0, 18.1, 18.2, 18.3, 18.4, 18.5, and 18.6 electrons per unit cell of $L1_0$ ordered FePt. The parameters for different levels of electron bandfilling are shown in table II. We note that, although the anisotropy values are calculated using ab-initio techniques, which are strictly valid at 0K, the atomistic model naturally introduces the temperature variation of anisotropy, which arises from thermally excited magnetization fluctuations.

III. RESULTS AND DISCUSSION

Based on the calculated values of K_u, which enter the atomistic model as site-resolved parameters, we study the magnetic switching properties of TEAMR and M-TEAMR structures at different width per thickness ratios (W/t), allowing investigation of the coercivity reduction due to the TEAMR effect, taking account of the specific localization of the anisotropy reduction characteristic of TEAMR and M-TEAMR. Here we concentrate on a study with a bit aspect ratio (BAR) of unity in order to clarify the degree of assist arising from the TEAMR effect. The 4×4, 8×8, 12×12, and 16×16 cells per bit of different bit sizes are studied firstly at 0K to investigate the reversal mechanism and a second series of calculations is performed to extend the study to a temperature of 300K. Coercivities of all bit sizes are calculated for 0.5, 1, and 2 of W/t ratios. We simulate both structures in figure 1(B) and 1(D) by modeling 2 different cases; firstly $L1_0$ ordered FePt, without trapping electron assist and secondly FePt subject to an electric field generating a bandfilling of n_{eff} = 18.38 per unit cell.

Finally we study the dependence of the hysteresis loop on the thermal stability factor (K_uV/k_BT) at room temperature (300K). Sizes of 4×4×8 (1.6×1.6×3.2 nm^3) and 10×10×15 (4×4×6 nm^3) cells per bit of BPM, TEAMR, and M-TEAMR structure are studied. The K_uV/k_BT values are 6.25 and 74.4 for the 4×4×8 and 10×10×15 cells bit size, respectively for which the M-H loops are compared.

We first consider the effects of different levels of bandfilling (induced by different applied voltages during the write process). Simulated hysteresis loops for different levels of electron bandfilling for the TEAMR structure at 4×4×8 cells per bit are shown in figure 2. For the intrinsic bandfilling of n_{eff} = 18.0 (equivalent to bulk FePt), the loop is very square owing to the uniaxial anisotropy and has a high coercivity of around 18T. Increasing the band filling reduces the coercivity due to the reduced effective anisotropy. The highest bandfilling gives a modest reduction of the intrinsic coercivity by around 11.7%.

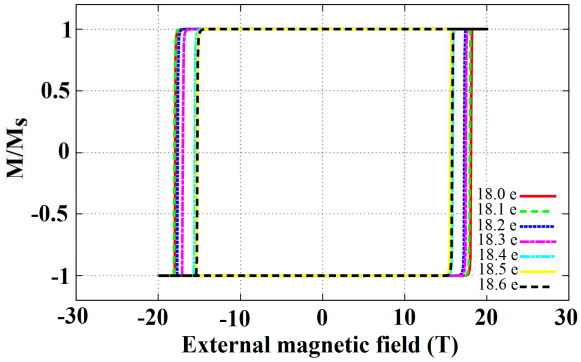

Fig. 2. M-H loops at different electron bandfillings in 4×4×8 cells per bit of TEAMR structure at T = 0K.

Figure 3 shows the M-H loops of modified TEAMR at different levels of electron bandfilling. For M-TEAMR the effect of bandfilling is much stronger. We can clearly see that the magnetic coercivity in M-TEAMR is lower than that of the TEAMR structure. The coercivity at 18.1, 18.2, 18.3, and 18.4 bandfillings decreases by 5.7%, 14.3%, 25.7%, and 60% of 18.0 intrinsic bandfilling, respectively. In addition the coercivity at 18.5 and 18.6 bandfillings is reduced by 72.4% relative to bulk FePt.

Figure 4 shows the percentage of magnetic switching reduction of TEAMR and M-TEAMR structures. The coercivity reduction of both structures decreases with increasing bit size. TEAMR results show that the magnetic switching reduction depends also on the change of W/t ratio while the magnetic switching reduction in M-TEAMR structures is independent of W/t ratio. However, the coercivity reduction of M-TEAMR is higher than TEAMR in all bit sizes and W/t ratios. The coercivity reduction of the M-TEAMR structure is as high as 60% while that of TEAMR is 12% for the 1.6×1.6 nm^2 bit and 0.5 of W/t ratio. Both results suggest that switching field reduction strongly depends on the number

of cells with enhanced n_{eff} relative to the total number of cells per bit of $L1_0$ ordered FePt [14].

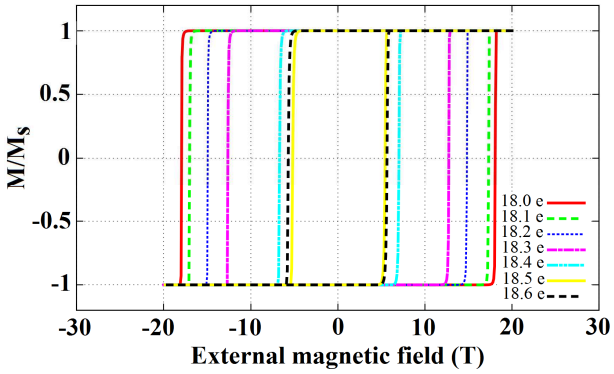

Fig. 3. M-H loops at different electron bandfillings in 4×4×8 cells per bit of modified TEAMR structure at T = 0K.

The degree of bandfilling achievable for a given electric field is determined by the dielectric constant of the material, suggesting the possible enhancement of bandfilling. In order to investigate the possible enhancement of the TEAMR effect, we calculate the number of electrons per unit cell for materials with increased dielectric constant using a finite element method simulator (COMSOL Multiphysics simulator). The simulation model is similar to [14] and here we show illustrative results for 16×16×8 and 16×16×16 cells per bit size. We apply 3 V-dc in the finite element model and calculate the number of electrons per unit cell in both sizes.

The results in figure 5 and 6 only show the number of electrons per unit cell at the side surface of modified TEAMR structure. Both results show that the number of electrons per unit cell in modified TEAMR increase with the dielectric constant or relative permittivity of the overcoat layer (OC).

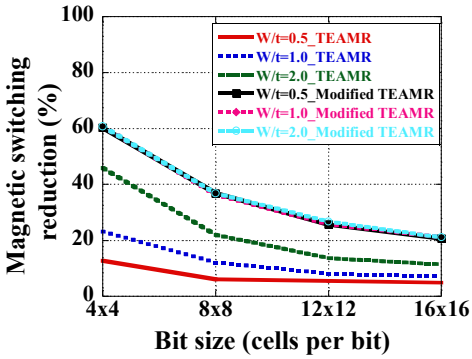

Fig. 4. Percentage of magnetic switching reduction in TEAMR and modified TEAMR structures at different bit sizes and *W/t* ratios.

For the 16×16×8 cells per bit structure, with a relative permittivity of the overcoat greater than 10, the number of electrons per unit cell is over 0.38 electron per unit cell while for the 16×16×16 cells per bit size, the same number per unit cell is achieved with a relative permittivity greater than 20. These results clearly show that the number of electrons per unit cell in the bigger bit can be enhanced by altering the relative permittivity of the overcoat, with consequently an important enhancement of the TEAMR and M-TEAMR effects.

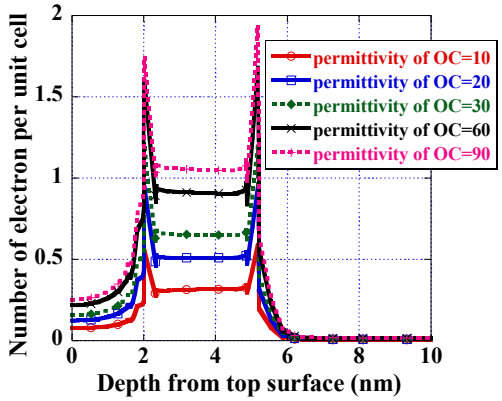

Fig. 5. Number of electrons per unit cell of modified TEAMR at the side surface in 6.4×6.4×3.2 nm^3 (16×16×8 cells per bit) bit.

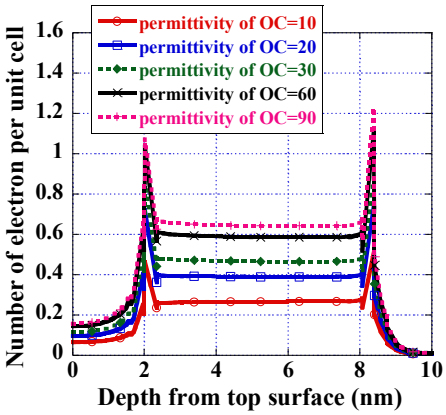

Fig. 6. Number of electrons per unit cell of modified TEAMR at the side surface in 6.4×6.4×6.4 nm^3 (16×16×16 cells per bit) bit.

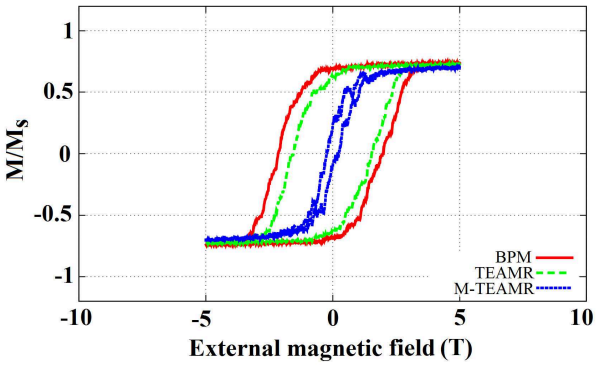

Fig. 7. M-H loops in 4×4×8 cells per bit of 3 structures at T = 300K.

Finally we study the magnetic properties at room temperature. Figure 7 shows the M-H loops of 3 structures at different thermal stability (K_uV/k_BT) value. The coercivity is reduced from the 0K value due to the thermal effects arising in the magnetic material. We observe that the coercivity of M-TEAMR is approximately 4 times lower than that of the TEAMR structure.

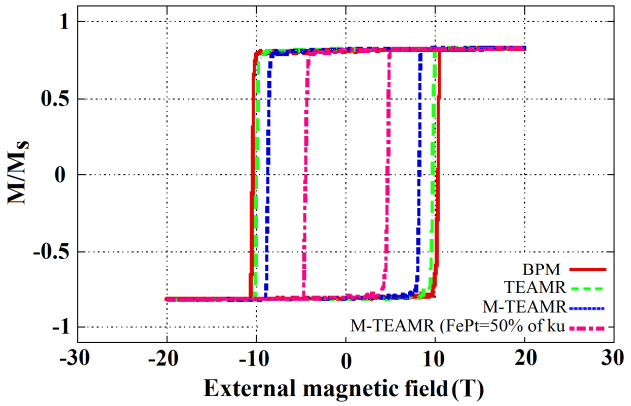

Fig. 8. M-H loops in 16×16×32 cells per bit of 3 structures at T = 300K.

Figure 8 shows that the coercivity of M-TEAMR is also lower than that of TEAMR and the M-H loops shown in figure 8 appear to be more square than figure 7 because the K_uV/k_BT of 16×16×32 cells per bit is much higher (399.36). Although the switching field reduction of M-TEAMR is larger for smaller bit size, the coercivity of M-TEAMR appears to be lower than the TEAMR structure for all bit sizes. However, the coercivity of M-TEAMR is still high due to high magnetic anisotropy of FePt. The switching field can be reduced if the magnetic anisotropy is lower. This is shown on figure 8 (pink dash line). The coercivity clearly can reduce to 4T by reducing K_u of FePt by 50%, which could be achieved by alloying.

IV. Conclusion

Electron Assisted Magnetic Recording enhancement by using a dielectric underlayer is confirmed by M-H loops studied using the VAMPIRE atomistic simulation package. The coercivity reduction is shown to be strongly dependent on the penetration depth of the bandfilling enhancement, which is limited due to the conductivity of FePt. The results show that the magnetic reduction depends strongly on the electron bandfilling of $L1_0$ ordered FePt. The magnetic switching reduction of M-TEAMR is independent on *W/t* ratio while that of TEAMR increases as the *W/t* ratio increases. In addition, the switching field reduction is larger if the bit size is smaller for both structures because of the larger relative volume over which the anisotropy reduction can be achieved. Note that the magnetic switching reduction in M-TEAMR is greater than that of TEAMR structure for all bit sizes. The coercivity with low K_uV/k_BT value is smaller than that with high K_uV/k_BT value due to thermal effect arising in the magnetic material at room temperature. The results show that the coercivity of M-TEAMR is approximately 4 times lower than that of TEAMR. Overall, the coercivity reduction due to bandfilling effects is apparently modest due to the nature of FePt as a conductor, which limits the increase of bandfilling to the surfaces of the material. This is especially the case for the larger bits. M-TEAMR is effective in extending the volume of the grain over which the anisotropy can be reduced. We also show that significant increases in bandfilling can be achieved by the use of materials with increased dielectric constant.

Acknowledgment

The authors would like to thank King Mongkut's University of Technology Thonburi and Seagate Technology (Thailand) for supporting this work. The authors wish to thank all members of Computational Magnetism Group at University of York for their help throughout the course of this work. In addition, this research work has been financially supported by University of York and Thailand Research Fund through the Royal Golden Jubilee Ph.D. Program (Grant No. PHD/0115/2553).

References

[1] Mark Gubbins. (2014, May 20). *Data Storage and HAMR* [online]. Available: http://www.photonics21.org/uploads/nEL1xYhSr6.pdf
[2] Andrew Baxter. (2014, May 5). *SSD vs HDD* [online]. Available: http://www.storagereview.com/ssd_vs_hdd
[3] L. Pan and D.B. Bogy, "Data storage: heat-assisted magnetic recording," *Nat. Photonics*, vol. 3, pp. 189-190, 2009.
[4] K. Matsumoto, A. Inomata, and S. Hasegawa, "Thermally assisted magnetic recording," *Fujitsu Sci. Tech. J.*, vol. 42, no. 1, pp. 158-167, Jan. 2006.
[5] Z.R. Dai, Shouheng Sun, and Z.L. Wang, "Phase transformation, coalescence, and twinning of monodisperse FePt nanocrystals," *Nano Lett.*, vol. 1, no. 8, pp. 443-447, 2001.
[6] A. Perumal, Y. K. Takahashi, and K. Hono, "$L1_0$ FePt–C nanogranular perpendicular anisotropy films with narrow size distribution," *Appl. Phys. Express 1*, 101301, 2008.
[7] J. T. Zhu, J. Zhu, and Y. Tang, "Microwave assisted magnetic recording," *IEEE Trans. Magn.*, vol. 44, no. 1, pp. 125–131, 2008.
[8] M. H. Kryder, E. C. Gate, T. W. Mcdaniel, W. A. Challener, R. E. Rottmayer, G. Ju, Y. T. Hsia, M. F. Erden, "Heat assisted magnetic recording," *Proc. IEEE*, vol. 96, no. 11, pp. 1810-1835, 2008.
[9] R. H. Victora and X. Shen, Exchange coupled composite media for perpendicular magnetic recording," *IEEE Trans. Magn.*, vol. 41, no. 10, pp. 2828-2833, 2005.
[10] T. Zhou, Z. Yuan, S. H. Leong, B. H. Low, C. L. Ong, L. Wang, B. Liu, C. M. Cheong, and S. Hu, "Trapping electron assisted magnetic recording," *IEEE Trans. Magn.*, vol. 46, no. 3, pp. 738–743, 2010.
[11] T. Zhou, S. H. Leong, Z. M. Yuan, S. B. Hu, C. L. Ong, and B. Liu, "Manipulation of magnetic by electrical field in real recording system," *Appl. Phys. Lett. 96*, 012506, 2010.
[12] M. Weisheit, S. Fähler, A. Marty, Y. Souche, C. Poinsignon, and D. Givord, "Electric field-induced modification of magnetic in thin-film ferromagnetic," *Sci.*, vol. 315, no. 5810, pp. 349-351, 2007.
[13] R. Cuadrado, Timothy J. Klemmer, and R. W. Chantrell, "Magnetic anisotropy of Fe_1-y X_y Pt-L10 [X=Cr, Mn, Co, Ni, Cu] bulk alloys," *Phys. Lett. 105*, 152406, 2014.
[14] S. Aksornniem, M. Vopson, and R. Silapunt, "Trapping electron-assisted magnetic recording enhancement via dielectric underlayer media," *IEEE Trans. Magn.*, vol. 50, no. 10, 3101005, 2014.
[15] R. F. L. Evans, W. J. Fan, P. Chureemart, T. A. Ostler, M. O. A. Ellis, and R. W. Chantrell, "Atomistic spin model simulations of magnetic nanomaterials," *J. Phys.: Condens Matter*, 103202, 2014.
[16] B. Varaprasad, B. Y. Takahashi, and K. Hono, "Microstructure Control of L1-Ordered FePt Granular Film for Heat-Assisted Magnetic Recording (HAMR) Media," *J. Minerals, Metals & Materials Society*, vol. 65, 2013.
[17] R. F. L. Evans. (2014, April 2). *VAMPIRE Atomistic simulation of magnetic nanomaterial* [online]. Avaliable: http://vampire.york.ac.uk
[18] A. Lyberatos, D.V. Berkov, and R.W. Chantrell, "A method for the numerical simulation of the thermal magnetization fluctuations in micromagnetics," *J.Phys.: Condens Matter 5*, 8911-20, 1993.
[19] J. A. Garcia-Palacios and F. J. Lazaro, "Langevin-dynamics study of the dynamical properties of small magnetic particles," *Phys. Rev. B.*, vol. 58, 14937, 1998.

Magnetic Switching in BPM, TEAMR, and Modified TEAMR by Using Dielectric Underlayer Media

Suttipan Aksornniem[1,2], Richard F. L. Evans[2], Roy W. Chantrell[2], Rardchawadee Silapunt[1]

[1]Department of Electronic and Telecom. Eng., King Mongkut's University of Technology Thonburi, Bangkok, 10140, Thailand
[2]Department of Physics, University of York, Heslington, York, YO10 5DD, UK

In this paper we study the coercivity of Bit Patterned Media (BPM), Trapping Electron Assisted Magnetic Recording (TEAMR), and modified TEAMR media by using a dielectric underlayer. The VAMPIRE magnetic simulator is used to model 3 structures of recording bits and to study the M-H loops using an atomistic spin model. The results show that the magnetic switching reduction in modified TEAMR and TEAMR depends on the bit size. The percentage of magnetic switching reduction in modified TEAMR is also larger than TEAMR for all bit sizes. For a bit size of 1.6×1.6×3.2 nm^3, the percentage of magnetic switching reduction in modified TEAMR is approximately 4 times higher than that in TEAMR.

***Index Terms*—magnetic data storage device; electron trapping assisted recording; TEAMR; VAMPIRE magnetic simulator; atomistic spin model.**

I. Introduction

HARD DISK drives are currently used to store over 90% of the world's digital data [1]. One main advantage of magnetic data storage is a much lower cost compared to any other technology, being approximately four times cheaper than equivalent solid state storage [2]. Recent developments in hard disk drives have seen improved areal density and energy efficiency. Presently, Perpendicular Magnetic Recording (PMR) technology is the dominant technology used in hard disk drives. However the areal density of conventional PMR is running into a limit of around 1 Tbpsi [3]. Areal density is limited by the requirement to retain thermal stability of written bits. Thermal stability cannot be maintained if the grain size is reduced below a critical limit where the magnetic anisotropy energy (K_uV/k_BT) is less than 60 [4]. The V and K_u represent the grain volume and magnetic anisotropy energy of the recording media respectively, k_B is the Boltzmann constant and T is the temperature. To obtain high thermal stability, the recording medium should have a high magnetic anisotropy energy. A favored candidate material is $L1_0$ ordered FePt with $K_u = 7\times10^6$ J/m^3 [5-6]. However, for such high anisotropy values the associated magnetic field required to write the data is greater than that available in conventional write heads.

Novel recording methods have been suggested to reduce the coercivity of the medium during the writing process. Examples include Microwave Assisted Magnetic Recording (MAMR) [7], Heat Assisted Magnetic Recording (HAMR) [8], and Exchange Coupled Composite (ECC) media [9]. Here we study Trapping Electron Assisted Magnetic Recording (TEAMR) [10]. Previously, trapping electron effect was demonstrated in CoCrPt-TiO_2 [11]. A low voltage (3 V_{dc}) was sufficient to create an electric field strong enough to trap 0.15 electron per cobalt atom in grain boundaries of media. That can reduce 13% of applied magnetic field reduction [11]. In addition, the first demonstration of electric field modified FePt properties in [12] showed that the magnetocrystalline anisotropy of FePt can be changed by an applied electric field. The method works by inducing electron filling in the valence band of $L1_0$ ordered FePt by applying a dc-voltage during the writing process [10] resulting in a change of the bandfilling to an effective number of electrons n_{eff}. By using Density Functional Theory (DFT) calculations [10] of the electron filling it was found that n_{eff} = 18.38 for $L1_0$ ordered FePt reduces the magnetic anisotropy energy (K_u) to zero. It was also found in [10] that the saturation magnetization (M_S) depended on n_{eff}. Recently [13] the alloying approach was studied theoretically using DFT, giving very good agreement with experimental data. In [13] the approach used was to model the actual alloy structures including structural relaxation. This goes beyond rigid the band model of [10] and suggests that the alloying approach does not give the exact dependence of K_u on n_{eff} in relation to TEAMR.

Recent simulations of TEAMR using finite element simulations demonstrated the capability of an electric field to induce electron filling in $L1_0$ ordered FePt [10]. However, it was found that the electric field gives rise to a rather localized change in the magnetocrystalline anisotropy. The calculations showed that bandfilling enhancement in a TEAMR structure only occurs close to the surface of an $L1_0$ ordered FePt recording bit because $L1_0$ ordered FePt is a conductor. Applying an external field directly makes it difficult to add electrons deep within the $L1_0$ ordered FePt film and so this effect can only reduce the anisotropy on the top surface of the bit. Therefore the reduction of the magnetic switching field was found to be only around 10%. A revised recording method known as modified TEAMR (M-TEAMR) uses a dielectric layer to induce surface charges at the side of the grain [14]. Using a finite element simulator it was predicted that the electron bandfilling increased deep inside the $L1_0$ ordered FePt layer. Although the bandfilling remains localized to the intergranular dielectric layer, the magnetocrystalline anisotropy is reduced within a larger volume of the grain than with normal TEAMR.

Here we study the magnetic switching of $L1_0$ ordered FePt bit patterned media (BPM), using TEAMR, and M-TEAMR

Manuscript received xx x, xxxx; revised xx x, xxxx; accepted xx x, xxxx. Date of publication xx x, xxxx; date of current version xx x, xxxx.
Corresponding author: R. Silapunt (e-mail: rardchawadee.sil@kmutt.ac.th).
Color versions of one or more of the figures in this paper are available online at http://ieeexplore.ieee.org.

by introducing a dielectric underlayer. The magnetic switching of the 3 structures is investigated using an atomistic spin model, which has the required spatial resolution to investigate the effects of local reduction of the magnetocrystalline anisotropy.

II. Theoretical Model

The magnetic properties are investigated using an atomistic spin model [15] where the energetics of the system are described by the following spin Hamiltonian ($\mathcal{H}$).

$$\mathcal{H} = \mathcal{H}_{exc} + \mathcal{H}_{ani} + \mathcal{H}_{app} \tag{1}$$

Denoting terms for the exchange interaction, magnetic anisotropy, and externally applied magnetic field respectively. The bulk material parameters are chosen to be representative of $L1_0$ ordered FePt, a strong candidate for next generation magnetic recording technology [16]. The contributions to the Hamiltonian, given below, consist of terms representing exchange in the Heisenberg form, uniaxial anisotropy and a Zeeman term giving the interaction with the externally applied field.. These terms are;

$$\mathcal{H}_{exc} = -\sum_{i \neq j} J_{ij} \hat{S}_i \cdot \hat{S}_j \tag{2}$$

$$\mathcal{H}_{ani}^{uni} = k_u \sum_i (\hat{S}_i \cdot \hat{e}_i)^2 \tag{3}$$

$$\mathcal{H}_{app} = -\sum_i \mu_s \hat{S}_i \cdot \hat{H}_{app} \tag{4}$$

where J_{ij} = 3.28×10^{-21} J/link is the nearest neighbor exchange interaction, $\hat{S}_i$ and $\hat{S}_j$ are unit vectors representing the local and neighboring spin directions, k_u is the uniaxial anisotropy constant, μ_s is the atomic spin moment, and $\hat{H}_{app}$ is the externally applied field. The effect of bandfilling is modeled by considering its effect on the local anisotropy and atomic spin moment [10].

We carry out calculations using the VAMPIRE atomistic modelling package [17], in which the magnetization dynamics of the system are included via the use of the LLG equation given by;

$$\frac{\partial \hat{S}_i}{\partial t} = -\frac{\gamma_i}{(1+\lambda_i^2)} (\hat{S}_i \times (\hat{H}_i + \lambda_i \hat{S}_i \times \hat{H}_i)) \tag{5}$$

Here λ_i and γ_i are the microscopic thermal bath coupling parameter and the gyromagnetic ratio respectively. The effective field on each spin is then given by $-d\mathcal{H}/dS_i$ where S_i is the magnetic moment of the site, *i*. To introduce the effects of temperature the local field is enhanced by a stochastic term, which describes the coupling of the spin system to the external thermal bath. The thermal fluctuations are included as a white noise term, uncorrelated in time and space, which is added into the effective field [18]. The stochastic integrals are interpreted as Stratonovich integrals [19]. The moments of the stochastic process are defined through fluctuation dissipation theory as:

$$\left\langle \varsigma_i^a(t) \varsigma_j^b(t) \right\rangle = 2\delta_{ij}\delta_{ab}(t-t') \frac{\lambda_i k_B T}{\mu_i \gamma_i} \tag{6}$$

$$\left\langle \varsigma_i^a(t) \right\rangle = 0 \tag{7}$$

Here *a, b* are Cartesian components and *T* is the temperature of the thermal bath to which the spins are coupled. The coupling of the spins to the thermal bath (λ_i) is a parameter which attempts to describe all of the energy and momentum transfer channels into the spin system, for example from the conduction electrons or the lattice.

This paper studies the coercivity of magnetic recording media of 3 structural types. These are BPM, TEAMR, and M-TEAMR including a dielectric underlayer. The 3 structures are shown in figure 1(B), 1(C), and 1(D). Figure (C) and (D) illustrate the major difference between TEAMR and M-TEAMR where coloring indicates the parts of the grain where the anisotropy is reduced due to the bandfilling. A recording grain consists of several unit cells of $L1_0$ ordered FePt. The cell size of $L1_0$ ordered FePt is 3.864 Å (c/a =0.96) that is shown in figure 1(A).

The aim is to investigate the effect on the coercivity of the degree of bandfilling, the width/thickness ratio (*W/t*) of the bits and the thermal stability value.

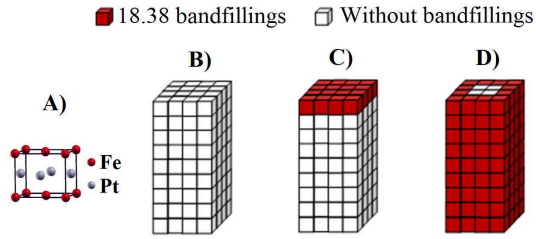

Fig. 1. Structures of A) $L1_0$ ordered FePt unit cell, B) BPM, C) TEAMR, and D) M-TEAMR by using dielectric underlayer, where the coloring indicates the parts of the grain where the anisotropy is reduced due to the bandfilling.

The recording bit of a BPM structure consists of many $L1_0$ ordered FePt unit cells that is shown schematically in figure 1(B). The bandfilled electron unit cells in the TEAMR structure (indicated by the colored cells) only occur at the top surface of $L1_0$ ordered FePt bit while the M-TEAMR structure gives rise to bandfilling at the side surface of the $L1_0$ ordered FePt grain. TEAMR and M-TEAMR structures are shown in figure 1(C) and 1(D), respectively. The material parameters used in the simulations are given in table I. Note that the exchange energy is independent of a number of bandfilling electron but on Boltzmann's constant and a number of nearest neighbor atoms.

K_u without bandfilling in $L1_0$ ordered FePt is 8.57×10^6 J/m^3 and with n_{eff} = 18.38 in $L1_0$ ordered FePt, the value decreases to zero. The saturation magnetizations (M_s) are 1.0745×10^6 J/(T·K^3) and 1.025×10^6 J/(T·K^3) without and with 18.38 electron bandfilling in $L1_0$ ordered FePt [10], respectively.

TABLE I
MATERIAL PROPERTIES

Parameter	Material:$L1_0$ ordered FePt	
	No bandfilling	18.38 bandfilling
Unit cell size, a	3.864 Å	3.864 Å
Unit cell size, c	3.748 Å	3.748 Å
Anisotropy energy	$1.2\text{x}10^{-22}$ J/atom	0 J/atom
Exchange energy	$3.28\text{x}10^{-21}$ J/link	$3.28\text{x}10^{-21}$ J/link
Atomic spin moment, μ_S	$1.62\mu_B$	$1.56\mu_B$

TABLE II
PARAMETERS AT DIFFERENT BANDFILLING

Bandfilling (e)	Material properties			
	K_u (J/m^3)	M_s (J/T·m^3)	μ_S (μ_B)	k_u (J/atom)
18.0	8.57×10^{6}	1.0745×10^{6}	1.620	1.198×10^{-22}
18.1	7.75×10^{6}	1.0631×10^{6}	1.603	1.084×10^{-22}
18.2	5.96×10^{6}	1.0528×10^{6}	1.588	8.337×10^{-23}
18.3	4.25×10^{6}	1.0431×10^{6}	1.573	5.945×10^{-23}
18.4	-0.47×10^{6}	1.0314×10^{6}	1.556	-6.575×10^{-24}
18.5	-1.64×10^{6}	1.0157×10^{6}	1.532	-2.294×10^{-23}
18.6	-1.29×10^{6}	0.9975×10^{6}	1.505	-1.804×10^{-23}

First we simulate different levels of electron bandfilling in TEAMR and modified TEAMR structures. The recording bits of TEAMR and modified TEAMR are modeled using the VAMPIRE simulator based on figure 1(C) and 1(D) respectively. The bit size is taken as 4×4×8 cells per bit (1.6×1.6×3.2 nm^3) in both structures. The initial simulations are carried out at 0K, which will allow comparison with micromagnetic simulations, followed by an investigation of the effect of temperature. The anisotropy and M_s values are calculated for electron bandfillings of n_{eff} = 18.0, 18.1, 18.2, 18.3, 18.4, 18.5, and 18.6 electrons per unit cell of $L1_0$ ordered FePt. The parameters for different levels of electron bandfilling are shown in table II. We note that, although the anisotropy values are calculated using ab-initio techniques, which are strictly valid at 0K, the atomistic model naturally introduces the temperature variation of anisotropy, which arises from thermally excited magnetization fluctuations.

III. RESULTS AND DISCUSSION

Based on the calculated values of K_u, which enter the atomistic model as site-resolved parameters, we study the magnetic switching properties of TEAMR and M-TEAMR structures at different width per thickness ratios (W/t), allowing investigation of the coercivity reduction due to the TEAMR effect, taking account of the specific localization of the anisotropy reduction characteristic of TEAMR and M-TEAMR. Here we concentrate on a study with a bit aspect ratio (BAR) of unity in order to clarify the degree of assist arising from the TEAMR effect. The 4×4, 8×8, 12×12, and 16×16 cells per bit of different bit sizes are studied firstly at 0K to investigate the reversal mechanism and a second series of calculations is performed to extend the study to a temperature of 300K. Coercivities of all bit sizes are calculated for 0.5, 1, and 2 of W/t ratios. We simulate both structures in figure 1(B) and 1(D) by modeling 2 different cases; firstly $L1_0$ ordered FePt, without trapping electron assist and secondly FePt subject to an electric field generating a bandfilling of n_{eff} = 18.38 per unit cell.

Finally we study the dependence of the hysteresis loop on the thermal stability factor (K_uV/k_BT) at room temperature (300K). Sizes of 4×4×8 (1.6×1.6×3.2 nm^3) and 10×10×15 (4×4×6 nm^3) cells per bit of BPM, TEAMR, and M-TEAMR structure are studied. The K_uV/k_BT values are 6.25 and 74.4 for the 4×4×8 and 10×10×15 cells bit size, respectively for which the M-H loops are compared.

We first consider the effects of different levels of bandfilling (induced by different applied voltages during the write process). Simulated hysteresis loops for different levels of electron bandfilling for the TEAMR structure at 4×4×8 cells per bit are shown in figure 2. For the intrinsic bandfilling of n_{eff} = 18.0 (equivalent to bulk FePt), the loop is very square owing to the uniaxial anisotropy and has a high coercivity of around 18T. Increasing the band filling reduces the coercivity due to the reduced effective anisotropy. The highest bandfilling gives a modest reduction of the intrinsic coercivity by around 11.7%.

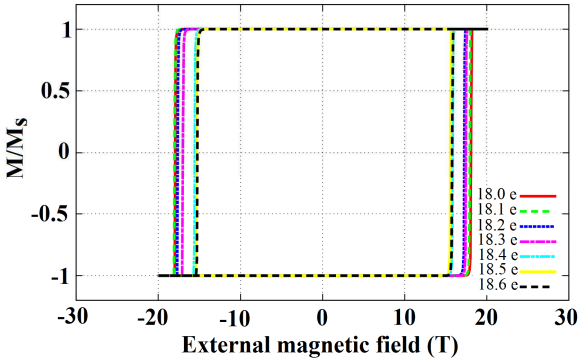

Fig. 2. M-H loops at different electron bandfillings in 4×4×8 cells per bit of TEAMR structure at T = 0K.

Figure 3 shows the M-H loops of modified TEAMR at different levels of electron bandfilling. For M-TEAMR the effect of bandfilling is much stronger. We can clearly see that the magnetic coercivity in M-TEAMR is lower than that of the TEAMR structure. The coercivity at 18.1, 18.2, 18.3, and 18.4 bandfillings decreases by 5.7%, 14.3%, 25.7%, and 60% of 18.0 intrinsic bandfilling, respectively. In addition the coercivity at 18.5 and 18.6 bandfillings is reduced by 72.4% relative to bulk FePt.

Figure 4 shows the percentage of magnetic switching reduction of TEAMR and M-TEAMR structures. The coercivity reduction of both structures decreases with increasing bit size. TEAMR results show that the magnetic switching reduction depends also on the change of W/t ratio while the magnetic switching reduction in M-TEAMR structures is independent of W/t ratio. However, the coercivity reduction of M-TEAMR is higher than TEAMR in all bit sizes and W/t ratios. The coercivity reduction of the M-TEAMR structure is as high as 60% while that of TEAMR is 12% for the 1.6×1.6 nm^2 bit and 0.5 of W/t ratio. Both results suggest that switching field reduction strongly depends on the number

of cells with enhanced n_{eff} relative to the total number of cells per bit of $L1_0$ ordered FePt [14].

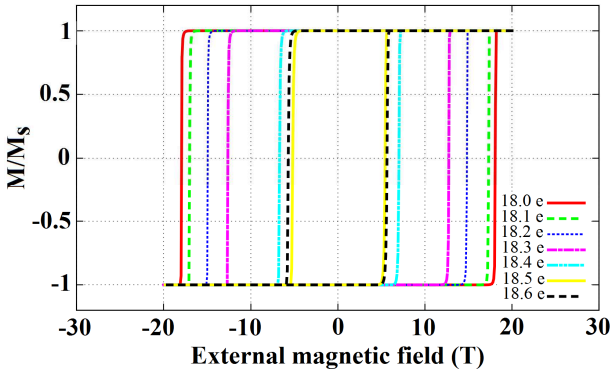

Fig. 3. M-H loops at different electron bandfillings in 4×4×8 cells per bit of modified TEAMR structure at T = 0K.

The degree of bandfilling achievable for a given electric field is determined by the dielectric constant of the material, suggesting the possible enhancement of bandfilling. In order to investigate the possible enhancement of the TEAMR effect, we calculate the number of electrons per unit cell for materials with increased dielectric constant using a finite element method simulator (COMSOL Multiphysics simulator). The simulation model is similar to [14] and here we show illustrative results for 16×16×8 and 16×16×16 cells per bit size. We apply 3 V-dc in the finite element model and calculate the number of electrons per unit cell in both sizes.

The results in figure 5 and 6 only show the number of electrons per unit cell at the side surface of modified TEAMR structure. Both results show that the number of electrons per unit cell in modified TEAMR increase with the dielectric constant or relative permittivity of the overcoat layer (OC).

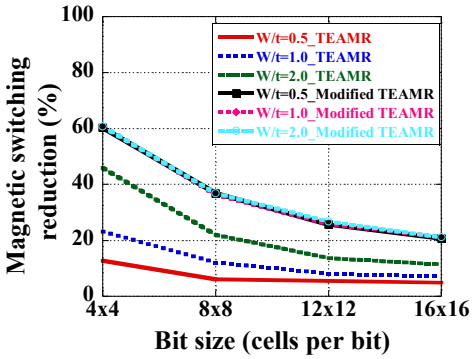

Fig. 4. Percentage of magnetic switching reduction in TEAMR and modified TEAMR structures at different bit sizes and *W/t* ratios.

For the 16×16×8 cells per bit structure, with a relative permittivity of the overcoat greater than 10, the number of electrons per unit cell is over 0.38 electron per unit cell while for the 16×16×16 cells per bit size, the same number per unit cell is achieved with a relative permittivity greater than 20. These results clearly show that the number of electrons per unit cell in the bigger bit can be enhanced by altering the relative permittivity of the overcoat, with consequently an important enhancement of the TEAMR and M-TEAMR effects.

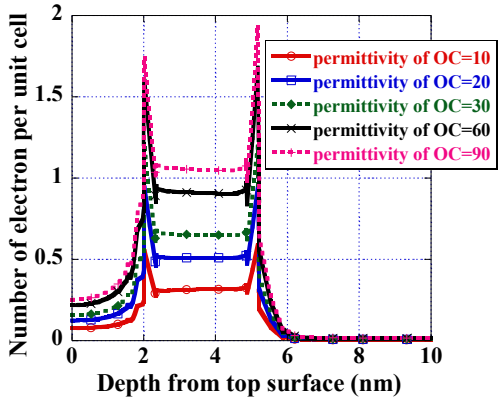

Fig. 5. Number of electrons per unit cell of modified TEAMR at the side surface in 6.4×6.4×3.2 nm^3 (16×16×8 cells per bit) bit.

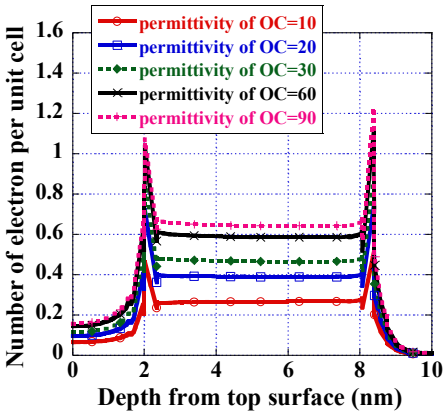

Fig. 6. Number of electrons per unit cell of modified TEAMR at the side surface in 6.4×6.4×6.4 nm^3 (16×16×16 cells per bit) bit.

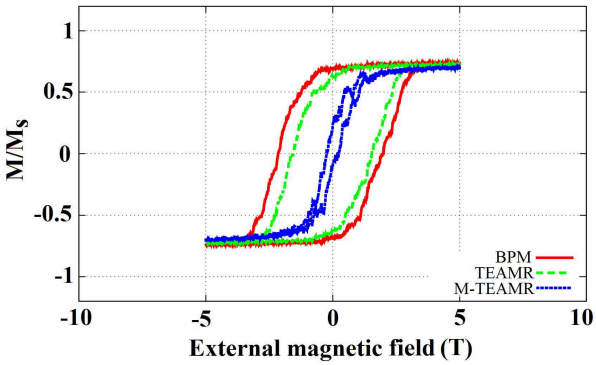

Fig. 7. M-H loops in 4×4×8 cells per bit of 3 structures at T = 300K.

Finally we study the magnetic properties at room temperature. Figure 7 shows the M-H loops of 3 structures at different thermal stability (K_uV/k_BT) value. The coercivity is reduced from the 0K value due to the thermal effects arising in the magnetic material. We observe that the coercivity of M-TEAMR is approximately 4 times lower than that of the TEAMR structure.

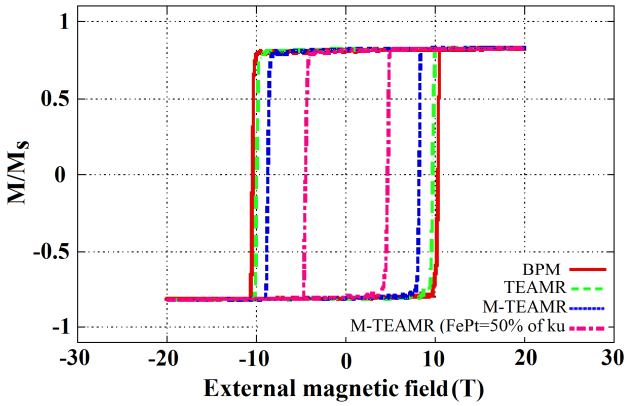

Fig. 8. M-H loops in 16×16×32 cells per bit of 3 structures at T = 300K.

Figure 8 shows that the coercivity of M-TEAMR is also lower than that of TEAMR and the M-H loops shown in figure 8 appear to be more square than figure 7 because the K_uV/k_BT of 16×16×32 cells per bit is much higher (399.36). Although the switching field reduction of M-TEAMR is larger for smaller bit size, the coercivity of M-TEAMR appears to be lower than the TEAMR structure for all bit sizes. However, the coercivity of M-TEAMR is still high due to high magnetic anisotropy of FePt. The switching field can be reduced if the magnetic anisotropy is lower. This is shown on figure 8 (pink dash line). The coercivity clearly can reduce to 4T by reducing K_u of FePt by 50%, which could be achieved by alloying.

IV. Conclusion

Electron Assisted Magnetic Recording enhancement by using a dielectric underlayer is confirmed by M-H loops studied using the VAMPIRE atomistic simulation package. The coercivity reduction is shown to be strongly dependent on the penetration depth of the bandfilling enhancement, which is limited due to the conductivity of FePt. The results show that the magnetic reduction depends strongly on the electron bandfilling of $L1_0$ ordered FePt. The magnetic switching reduction of M-TEAMR is independent on *W/t* ratio while that of TEAMR increases as the *W/t* ratio increases. In addition, the switching field reduction is larger if the bit size is smaller for both structures because of the larger relative volume over which the anisotropy reduction can be achieved. Note that the magnetic switching reduction in M-TEAMR is greater than that of TEAMR structure for all bit sizes. The coercivity with low K_uV/k_BT value is smaller than that with high K_uV/k_BT value due to thermal effect arising in the magnetic material at room temperature. The results show that the coercivity of M-TEAMR is approximately 4 times lower than that of TEAMR. Overall, the coercivity reduction due to bandfilling effects is apparently modest due to the nature of FePt as a conductor, which limits the increase of bandfilling to the surfaces of the material. This is especially the case for the larger bits. M-TEAMR is effective in extending the volume of the grain over which the anisotropy can be reduced. We also show that significant increases in bandfilling can be achieved by the use of materials with increased dielectric constant.

Acknowledgment

The authors would like to thank King Mongkut's University of Technology Thonburi and Seagate Technology (Thailand) for supporting this work. The authors wish to thank all members of Computational Magnetism Group at University of York for their help throughout the course of this work. In addition, this research work has been financially supported by University of York and Thailand Research Fund through the Royal Golden Jubilee Ph.D. Program (Grant No. PHD/0115/2553).

References

[1] Mark Gubbins. (2014, May 20). *Data Storage and HAMR* [online]. Available: http://www.photonics21.org/uploads/nEL1xYhSr6.pdf
[2] Andrew Baxter. (2014, May 5). *SSD vs HDD* [online]. Available: http://www.storagereview.com/ssd_vs_hdd
[3] L. Pan and D.B. Bogy, "Data storage: heat-assisted magnetic recording," *Nat. Photonics*, vol. 3, pp. 189-190, 2009.
[4] K. Matsumoto, A. Inomata, and S. Hasegawa, "Thermally assisted magnetic recording," *Fujitsu Sci. Tech. J.*, vol. 42, no. 1, pp. 158-167, Jan. 2006.
[5] Z.R. Dai, Shouheng Sun, and Z.L. Wang, "Phase transformation, coalescence, and twinning of monodisperse FePt nanocrystals," *Nano Lett.*, vol. 1, no. 8, pp. 443-447, 2001.
[6] A. Perumal, Y. K. Takahashi, and K. Hono, "$L1_0$ FePt–C nanogranular perpendicular anisotropy films with narrow size distribution," *Appl. Phys. Express 1*, 101301, 2008.
[7] J. T. Zhu, J. Zhu, and Y. Tang, "Microwave assisted magnetic recording," *IEEE Trans. Magn.*, vol. 44, no. 1, pp. 125–131, 2008.
[8] M. H. Kryder, E. C. Gate, T. W. Mcdaniel, W. A. Challener, R. E. Rottmayer, G. Ju, Y. T. Hsia, M. F. Erden, "Heat assisted magnetic recording," *Proc. IEEE*, vol. 96, no. 11, pp. 1810-1835, 2008.
[9] R. H. Victora and X. Shen, Exchange coupled composite media for perpendicular magnetic recording," *IEEE Trans. Magn.*, vol. 41, no. 10, pp. 2828-2833, 2005.
[10] T. Zhou, Z. Yuan, S. H. Leong, B. H. Low, C. L. Ong, L. Wang, B. Liu, C. M. Cheong, and S. Hu, "Trapping electron assisted magnetic recording," *IEEE Trans. Magn.*, vol. 46, no. 3, pp. 738–743, 2010.
[11] T. Zhou, S. H. Leong, Z. M. Yuan, S. B. Hu, C. L. Ong, and B. Liu, "Manipulation of magnetic by electrical field in real recording system," *Appl. Phys. Lett. 96*, 012506, 2010.
[12] M. Weisheit, S. Fähler, A. Marty, Y. Souche, C. Poinsignon, and D. Givord, "Electric field-induced modification of magnetic in thin-film ferromagnetic," *Sci.*, vol. 315, no. 5810, pp. 349-351, 2007.
[13] R. Cuadrado, Timothy J. Klemmer, and R. W. Chantrell, "Magnetic anisotropy of Fe_1-y X_y Pt-L10 [X=Cr, Mn, Co, Ni, Cu] bulk alloys," *Phys. Lett. 105*, 152406, 2014.
[14] S. Aksornniem, M. Vopson, and R. Silapunt, "Trapping electron-assisted magnetic recording enhancement via dielectric underlayer media," *IEEE Trans. Magn.*, vol. 50, no. 10, 3101005, 2014.
[15] R. F. L. Evans, W. J. Fan, P. Chureemart, T. A. Ostler, M. O. A. Ellis, and R. W. Chantrell, "Atomistic spin model simulations of magnetic nanomaterials," *J. Phys.: Condens Matter*, 103202, 2014.
[16] B. Varaprasad, B. Y. Takahashi, and K. Hono, "Microstructure Control of L1-Ordered FePt Granular Film for Heat-Assisted Magnetic Recording (HAMR) Media," *J. Minerals, Metals & Materials Society*, vol. 65, 2013.
[17] R. F. L. Evans. (2014, April 2). *VAMPIRE Atomistic simulation of magnetic nanomaterial* [online]. Avaliable: http://vampire.york.ac.uk
[18] A. Lyberatos, D.V. Berkov, and R.W. Chantrell, "A method for the numerical simulation of the thermal magnetization fluctuations in micromagnetics," *J.Phys.: Condens Matter 5*, 8911-20, 1993.
[19] J. A. Garcia-Palacios and F. J. Lazaro, "Langevin-dynamics study of the dynamical properties of small magnetic particles," *Phys. Rev. B.*, vol. 58, 14937, 1998.